

Base from U.S. Geological Survey, 2019, Glade Valley, N.C., Sparta East, N.C., Sparta West, N.C., and Whitehead, N.C. Lateral hillshade derived from USGS Sparta earthquake data with lighting azimuth at 220° and 70° inclination. Universal Transverse Mercator projection, zone 17 North. North American Datum of 1983.

SCALE 1:24 000

CONTOUR INTERVAL 40 FEET
NORTH AMERICAN VERTICAL DATUM OF 1988

MAP LOCATION

Geos mapped in 2021 and 2022
GIS database by Benjamin R. Weinmann
Cartography by E. Allen Order Jr.
Edited by David A. Shields

Preliminary Map of the Surface Rupture From the August 9, 2020, Mw 5.1 Earthquake Near Sparta, North Carolina—The Little River Fault and Other Possible Coseismic Features

By
Arthur J. Merschat and Mark W. Carter
2023

EXPLANATION OF MAP SYMBOLS

FAULTS

[Where thrust faults are solid the location is certain and mapped within 0.5 meters; thrust faults shown with a long dash are approximate and located within 3 meters; thrust faults shown with a short dash are inferred and located within 5 meters. Faults are queried where existence or identity are questionable]

- Thrust fault with scarp—Sawtooth on upper plate; hatchures point downscarp
- Thrust fault—Sawtooth on upper plate
- Thrust fault, approximate (long dashed)—Sawtooth on upper plate
- Thrust fault, inferred (short dashed)—Sawtooth on upper plate
- Thrust fault, inferred (short dashed), queried—Sawtooth on upper plate
- Fault, approximate (long dashed), queried—Movement type unknown or unspecified

STRUCTURE MEASUREMENTS

[Structural measurements from bedrock and saprolite exposures; symbols may be combined, and point of intersection represents point of observation; symbols may be moved for cartographic purposes]

- Outcrop-scale fault
- Joint
- Metamorphic foliation
- Vein
- Axial surface
- Fold axis
- Mineral lineation
- Slickenside

OTHER FEATURES

- Ground cracks, fissures, and mass-wasting scarps—These include ground cracks and fissures on the coseismic scarp, associated with liquefaction in a sandbar, and at (or near) head scarps of coseismic mass-wasting landslides. Ground cracks and fissures extend for lengths of decimeters to meters and have openings of 0.1 to 1 centimeters (cm) wide. Mass-wasting scarps have 1 to 20 cm of vertical translation. Dip of these features could not be measured accurately and are not shown

Rockfall

Earthquake epicenters (U.S. Geological Survey, 2022)

- Magnitude less than 2.0
- Magnitude 2.0–4.0
- Magnitude 5.1 mainshock

ABSTRACT

This publication is a preliminary map and geodatabase of the coseismic surface rupture and other coseismic features generated from the August 9, 2020, Mw 5.1 earthquake near Sparta, North Carolina. Geologic mapping facilitated by analysis of post-earthquake quality level 0 to 1 lidar, document the coseismic surface rupture, named the Little River fault, and other coseismic features. The Little River fault is traced for approximately 4 kilometers and cuts the regional Paleozoic fabric (mean foliation, 063°/57°), and the dominant strike of joint sets are 0°–10°, 130°–150°, and 320°–340°. Individual fault strands occur in an en echelon pattern within an approximately 10-meter-wide zone. Trenches across the Little River fault document a thrust fault oriented 110°/45° with at least 10 centimeters (cm) of displacement. The Little River fault is marked by a flexure or scarp with a height of 5–30 cm and a local maximum height of 50 cm. Southwest-side-up displacement is consistent along the fault and indicates thrust kinematics. The strike of the Little River fault changes from 110° to 130° near Duncan Farm where it crosses Chestnut Grove Church Road (NC Rt. 1426). Although the surface expression of the fault terminates and (or) is imperceptible at both ends, deformation is still clear in residual surface maps showing the change between pre- and post-earthquake lidar elevations. Other coseismic features documented are rockfalls, ground cracks, fissures, lateral spreading on a sandbar, and mass-wasting scarps; several possible faults that were identified from lidar analyses strike E-W and oblique to the Little River fault.

INTRODUCTION

The August 9, 2020, Mw 5.1 earthquake in Sparta, North Carolina, generated the first documented coseismic surface rupture in the eastern United States, the Little River fault (Hill and others, 2020; Merschat and others, 2020; Figueiredo and others, 2022). Geologic mapping facilitated by analysis of post-earthquake quality level 0 to 1 (QLO to Q1L) lidar data that was acquired after the earthquake, document the coseismic surface rupture (U.S. Geological Survey, 2020; lidar data is available to download at https://rockyweb.usgs.gov/delivery/Datasets/Staged/Elevation/LPC/Projects/NC_SpartaEarthquake_2020_D21/NC_SpartaEQ_1_2020). This report is a preliminary map of the coseismic surface rupture and other coseismic features such as rockfalls, ground cracks, fissures, lateral spreading on a sandbar in the bed of the Little River, mass-wasting scarps, and other possible faults. Earthquake epicenters and structural measurements from bedrock and saprolite exposures within a buffered area 1 kilometer (km) from the Little River fault are shown for comparison. Preliminary detailed surficial and bedrock geologic

maps of the Sparta East, Sparta West, and parts of the Glade Valley and Whitehead 7.5-minute quadrangles showing the surface rupture and other coseismic features, are described in Merschat and others (2023a). The associated data release (Merschat and others, 2023b; <https://doi.org/10.5066/955SPGHH>) includes the map geodatabase, metadata, and results of lidar interpretation with a residual surface map.

DISCUSSION

The earthquake epicenter was located in polydeformed crystalline rocks of the Neoproterozoic to Cambrian Ashe and Alligator Back Metamorphic Suites in the eastern Blue Ridge (Rankin and others, 1972; Carter and Merschat, 2014; Raymond, 2015). The metamorphic suites are composed of metamorphosed siliciclastic rocks and intercalated mafic and ultramafic rocks. Map units and rock types are listed in the database but are not separated or shown on the map. Rock types include amphibolite, muscovite schist, and quartzofeldspathic mica gneisses mapped as metagraywacke, metagraywacke with quartz stringers, conglomeratic metagraywacke, and pinstriped metagraywacke, which the latter is common to the Alligator Back Metamorphic Suite. The regional Paleozoic structure (foliation) strikes NE-SW and dips moderately SE (fig. 1A). Mineral lineations plunge SE and SW, and most fold axes plunge SW and NE (fig. 1B). Ar^{40}/Ar^{39} hornblende and muscovite ages suggest the regional foliation formed at approximately 340 million years before present (Ma, mega annum) (Merschat and others, 2016; Levine and others, 2018). Brittle structures include joints and faults. Several faults strike WNW-ESE and dip SW, whereas the dominant joint set strikes 0°–10°, 130°–150°, and 320°–340° (fig. 1C, 1D).

The Little River fault is traced for approximately 4 kilometers with individual fault strands that occur in an en echelon pattern within an approximately 10 meter(n)-wide zone. Four shallow trenches (shown on map) excavated across the Little River fault document a thrust fault that is oriented with a strike and dip of 110°/45° (using right-hand rule; fig. 1A, 1C) and at least 10 centimeters (cm) of displacement (Hill and others, 2020; Figueiredo and others, 2022). The fault is marked by a flexure or scarp with a typical height of 5–30 cm and a local maximum height of 50 cm. Southwest-side-up displacement is consistent with thrust kinematics. The strike of the Little River fault changes from 110° to 130° near Duncan Farm (see map) where it crosses Chestnut Grove Church Road (NC Rt. 1426). Southeast of Duncan Farm, the surface expression of the fault is imperceptible, but deformation is still observed in raster subtraction of the 2016 QLO and 2020 QLO lidar datasets (see residual surface map, fig. 2) showing the change between pre- and post-earthquake lidar-derived elevations.

LIDAR ANALYSES, MAPPING, AND GEODATABASE

The mapped trace of the Little River fault, and other possible coseismic faults shown on the map sheet and in the geodatabase (see data release by Merschat and others, 2023b), use standard geologic map symbolization (Federal Geographic Data Committee, 2006) and database structure (U.S. Geological Survey National Cooperative Geologic Mapping Program, 2020). Post-earthquake QLO-Q1L data is available separately from this Open-File Report and database at https://rockyweb.usgs.gov/delivery/Datasets/Staged/Elevation/LPC/Projects/NC_SpartaEarthquake_2020_D21/NC_SpartaEQ_1_2020 (U.S. Geological Survey, 2020). Lidar analysis and interpretation involved (1) viewing a raster hillshade image derived from the lidar digital elevation model (DEM) with varying illumination; (2) comparing the 2016 QLO and 2020 QLO lidar-derived raster hillshade images; (3) creating percent slope maps; and (4) raster subtraction (fig. 3). Raster subtraction of the 2016 QLO and 2020 QLO lidar yielded a residual surface map that shows the change in elevation (figs. 2 and 3D). The Little River fault and other features were mapped with an iterative approach of lidar interpretation and field checks (fig. 4). Digital maps were loaded onto Apple iPads running the application Fieldmore. The iPads were either cell-enabled or used Bluetooth-enabled GPS receivers at 3-m accuracy (Department of Defense, 2020). Initial field observations that were carried out prior to the lidar analysis and interpretation mapped obvious portions of the Little River fault. Fieldwork then verified lidar-derived interpretations, identified non-coseismic features, and helped revise earlier versions of the surface rupture. Attribution of the Little River fault and related geologic features indicate the identity, existence, and location accuracy of the geologic features, as well as the surface deformation (for example, scarp versus blind or imperceptible surface deformation); these attributes were determined from integrated and iterative fieldwork and analysis of post-earthquake QLO lidar. Structures and features mapped from the QLO lidar (U.S. Geological Survey, [undated]; horizontal accuracy <0.35 m, <https://www.usgs.gov/3d-elevation-program/topographic-data-quality-levels-q1b>) and identified in the field are considered located within 0.5 m.

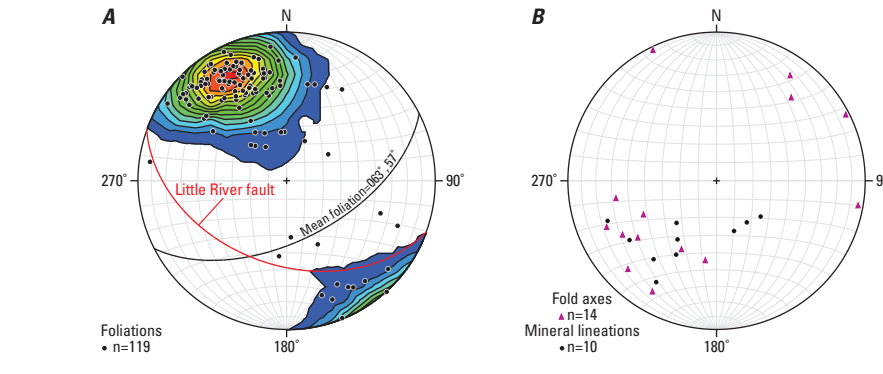


Figure 1. Stereonets (A–C) and rose diagram (D) showing structural data measured from bedrock and saprolite exposures of the Ashe and Alligator Back Metamorphic Suites within 1 kilometer of the Little River fault. A. Poles to Paleozoic foliation (black dots) in the Ashe and Alligator Back Metamorphic Suites. Kamb contour interval is 2 sigma; counting area is 7 percent of the stereonet area and the expected number of foliation measurements is 8.367 per contour. The mean Paleozoic foliation (063°, 57°; using right-hand rule) is plotted as a black great circle; the orientation of the Little River fault (measured in a trench) is plotted as a red great circle. B. Poles to mineral lineations (black dots) and fold axes (magenta triangles). C. Orientation of brittle faults (black great circles) and slickensides (black dots) measured in bedrock and saprolite. The orientation of the Little River fault is plotted as a red great circle. D. Rose diagram showing the strike of joints with the dominant joint set striking 0°–10°, 130°–150°, and 320°–340°. Petals are grouped within 10-degree classes, and the total number of measurements (n=111). The number of measurements (n) is indicated at the bottom of each diagram. Stereonets are lower hemisphere, equal-area projections and were plotted using the computer program Stereonet v. 9.2.3 (Allmendinger and Cardozo, 2015).

Approximate and inferred structures and features are mapped with a combination of QLO lidar and GPS (horizontal accuracy up to 3 m; Department of Defense, 2020) and are located within 3 and 5 m, respectively. Queried structures or features indicate the existence or identity is questionable.

The following seven classifications are used to map the Little River fault and other possible coseismic features.

Thrust fault with scarp

The coseismic surface rupture is identified on the ground and in lidar-derived hillshade raster images (fig. 3). The fault is marked by a 5- to 50-cm flexure or scarp with consistent southwest-side-up and thrust kinematics. Thrust kinematics was verified in several trenches across the rupture (trench locations are shown on map and are from Figueiredo and others, 2022). The existence and identity are certain; the location is mapped within 0.5 m. On the map, these faults are identified with solid lines with sawtooth on upper plate and hatchures that point downscarp.

Thrust fault

The coseismic fault is identified in the residual surface map showing the change between pre- and post-earthquake lidar elevations (fig. 2). Elevation changes across the scarp corroborate southwest-side-up thrust kinematics. Subtle scarp or other coseismic surface features are identified on the ground but cannot be mapped continuously. The existence and identity are certain; the location is mapped within 0.5 m. On the map, these faults are identified with solid lines with sawtooth on upper plate.

Thrust fault, approximate (long dashed)

The coseismic fault is identified in the residual surface map (fig. 2) showing the change between pre- and post-earthquake lidar elevations, but the distinction of the fault is not as clear in some locations. Elevation changes across the scarp corroborate southwest-side-up thrust kinematics. A few subtle coseismic surface features are identified on the ground but cannot be mapped continuously. The existence and identity are certain; the location is approximate and mapped within 3 m. On the map, these faults are identified with long dashes and sawtooth on the upper plate.

Thrust fault, inferred (short dashed)

The coseismic fault is identified in the residual surface map (fig. 2) showing the change between pre- and post-earthquake lidar elevations, but the distinction of the fault is not as clear or pronounced. Elevation changes across the scarp corroborate southwest-side-up thrust kinematics. Possible coseismic surface features on the ground are rare or ambiguous. The existence and identity are certain; the location is inferred and mapped within 5 m. On the map, these faults are identified with short dashes and sawtooth on the upper plate.

Thrust fault, inferred (short dashed), queried

These faults are identified through a similar process and criteria as “thrust fault, inferred”, however, there is less supporting evidence for the location. Changes in residual elevation across the feature (fig. 2) are significantly less than that of “thrust fault, inferred”; no surface deformation was identified, and there is less damage to buildings in the vicinity of the fault segments. The existence and identity are questionable. The location is inferred and mapped between 5–10 m. On the map, these faults are identified with short dashes, queries (?), and sawtooth on upper plate.

Fault, approximate (long dashed), queried

These possible coseismic faults and features are identified in the residual surface map (fig. 2) of the elevation change between pre- and post-earthquake lidar. Some faults and features may be directly related to the Little River fault or represent another possible fault striking oblique to the Little River fault. A few subtle surface features locally correspond with these faults. Changes in the residual elevation across the faults indicate southside-up movement consistent with thrust kinematics of the Little River fault. The existence and identity of the faults are questionable, the location is approximate and is mapped within 3 m. On the map, these faults are identified with long dashes and a query (?).

Ground cracks, fissures, and mass-wasting scarps

These point observations include several coseismic features mapped in the days and weeks following the main shock of the earthquake. These include ground cracks and fissures on the coseismic scarp, cracks associated with lateral spreading on a sandbar on the Little River near the trace of the Little River fault, and headscarps of coseismic mass-wasting slides. Ground cracks and fissures extend along strike from decimeters to meters and have openings of 0.1 to 3 cm

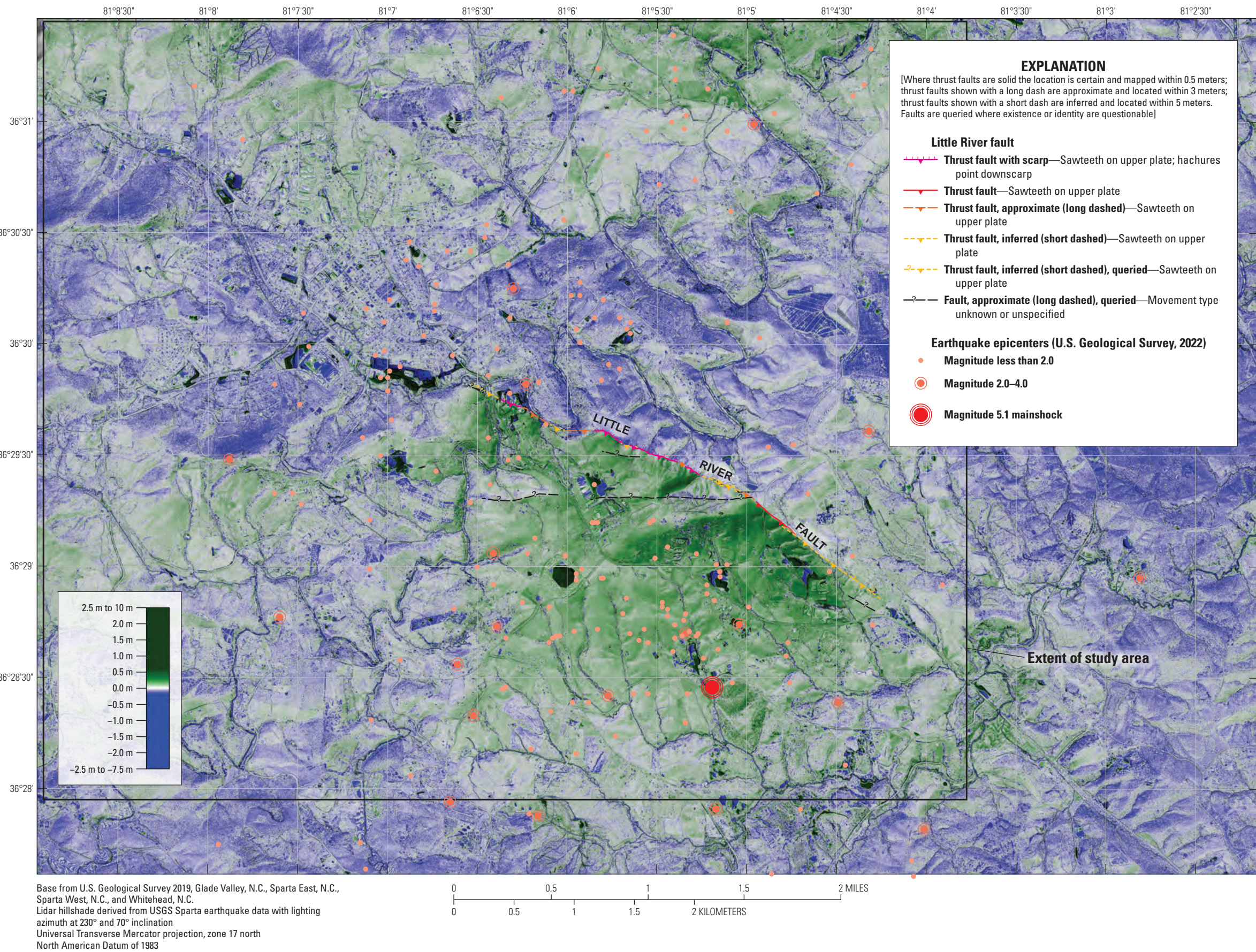


Figure 2. Residual surface map of 2016 lidar from the 2020 post-earthquake lidar showing the change in elevation in meters (m). Green indicates a positive change in elevation and blue indicates a negative change in elevation (see scale on left); the darkest colors are anthropogenic change (construction, buildings). The location of the Little River fault can be easily identified and is labeled. There is an approximately 11 square kilometer area of uplift on the hanging wall (southwest side) of the Little River fault. Other possible coseismic faults may exist including an E-W fault that may be 3 kilometers or longer but no surface deformation was observed along the fault trace.

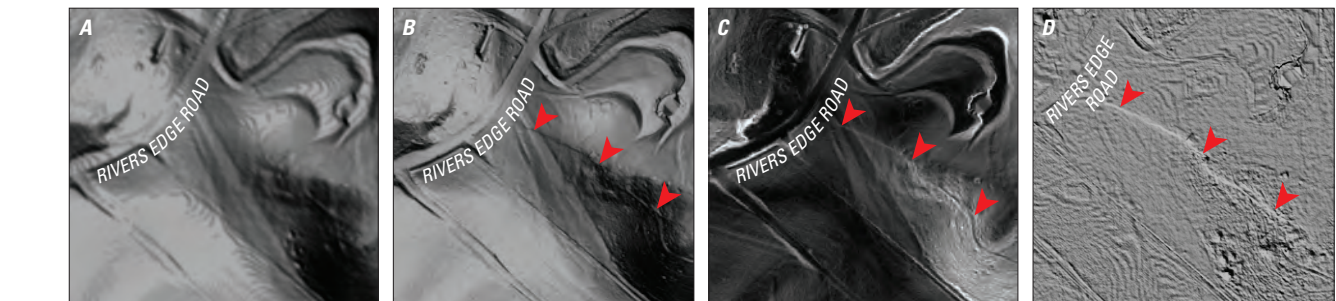


Figure 3. Lidar images showing the analyses involved (A) the comparison of 2016 lidar, (B) 2020 post-earthquake lidar, (C) percent slope map, and (D) raster subtraction. These analyses were used to trace the rupture across the landscape. Lidar images are all the same location along Rivers Edge Road where the fault buckled the road and ruptured a water main and continued across the pasture. Red arrows point to the surface rupture and are in the footwall of the Little River fault.

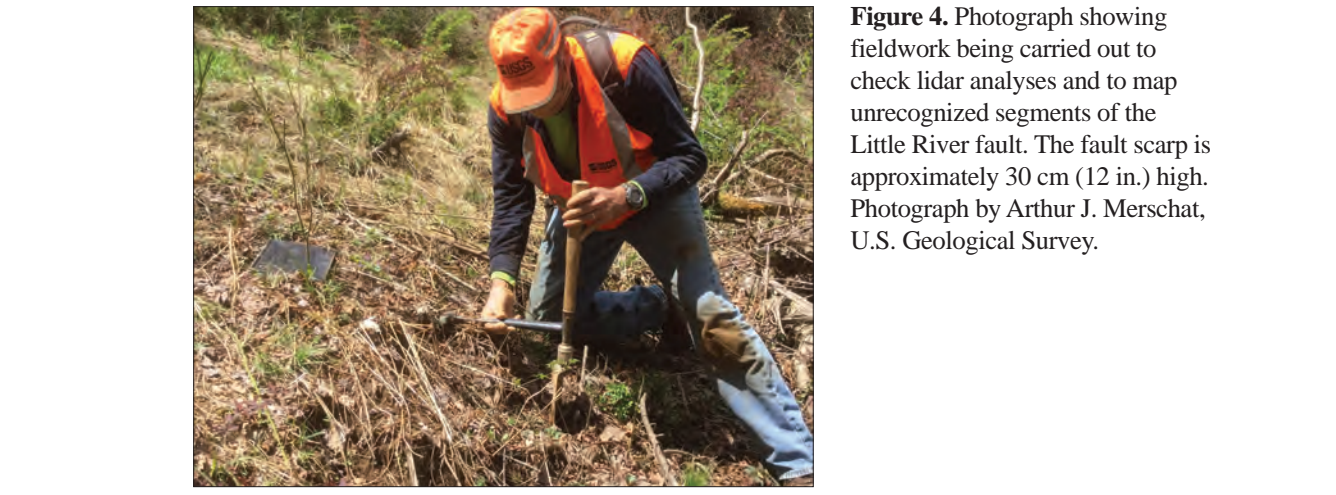


Figure 4. Photograph showing fieldwork being carried out to check lidar analyses and to map unrecognized segments of the Little River fault. The fault scarp is approximately 30 cm (12 in.) high. Photograph by Arthur J. Merschat, U.S. Geological Survey.

ACKNOWLEDGMENTS

Bedrock and surficial geologic mapping were supported by the U.S. Geological Survey (USGS) National Cooperative Geologic Mapping Program and the Earthquake Hazards Program. Funding for the post-earthquake lidar was from the USGS National Cooperative Geologic Mapping Program and the lidar was acquired through the USGS 3D Elevation Program and the National Geospatial Technical Operations Center. The following partners and collaborators are greatly appreciated for their assistance in mapping the surface rupture: Bart L. Cattannach, Jesse S. Hill, Thomas J. Douglas, Corey M. Scheip, and Richard M. Wooten of the North Carolina Geological Survey; Paula M. Figueiredo, Lewis A. Owen, Karl W. Wegmann, and Del R. Bohnenstiel of North Carolina State University; Kevin G. Stewart and Ashley S. Lynn of the University of North Carolina at Chapel Hill; and Anne C. Witt of the Virginia Geology and Mineral Resources Program. We would like to also acknowledge Bill C. Barton (USGS) and Greg J. Walsh (USGS) whose critical reviews significantly improved this publication.

REFERENCES CITED

Allmendinger, R., and Cardozo, N., 2015, Stereonet v. 9.3.2, computer program: software available at <https://www.rickallmendinger.net/stereonet/>.

Carter, M., and Merschat, A., 2014, Stratigraphy, structure, and regional correlation of eastern Blue Ridge sequences in southern Virginia and northwestern North Carolina—An interim report from new U.S. Geological Survey mapping, in Bailey, C.M., and Coiner, L.V., eds., Elevating geoscience in the southeastern United States: New ideas about old terranes—10-field guides for the GSA southeastern section meeting, Blacksburg, Virginia, 2014: Geological Society of America Field Guide 35, p. 215–241. [Also available at <https://doi.org/10.1130/2014.0035.07j>.]

Department of Defense, 2020, Global positioning system standard positioning service performance standard (5th ed.): Office of the Department of Defense, Washington D.C., 196 p., accessed August 4, 2022, at <https://www.gps.gov/technical/ps/2020-SPS-performance-standard.pdf>.

Federal Geographic Data Committee, 2006, FGDC digital cartographic standard for geologic map symbolization: Reston, Va., U.S. Geological Survey, Federal Geographic Data Committee, document number FGDC-STD-013-2006, 290 p., 2 pls. [Also available at https://ngmdb.usgs.gov/fgdc_gds/geolysmsd/download.php.]

Figueiredo, P.M., Hill, J.S., Merschat, A.J., Scheip, C.M., Stewart, K.G., Owen, L.A., Wooten, R.M., Carter, M.W., Szymanski, E., Horton, S.P., Wegmann, K.W., Bohnenstiel, D.R., Witt, A., Cattannach, B., and Douglas, T.J., 2022, The Mw 5.1 9 August, 2020, Sparta earthquake, North Carolina—The first documented seismic surface rupture in the eastern United States: Geological Society of America Today, v. 32, p. 4–11. [Also available at <https://doi.org/10.1130/GATG517A.1>.]

Hill, J.S., Carter, M.W., Cattannach, B.L., Douglas, T.J., Figueiredo, P.M., Kirby, E., Korte, D.M., Lynn, A.S., Merschat, A.J., Owen, L.A., Scheip, C.M., Stewart, K.G., Wells, S.B., Witt, A.C., and Wooten, R.M., 2020, Surface rupture of the Little River fault in response to the August 9, 2020 Mw 5.1 earthquake near Sparta, North Carolina [abs.]: AEG News, AEG2020 Virtual Conference Program with Abstracts, v. 63, no. 4, p. 16–17.

Levine, J.S.F., Merschat, A.J., McAleer, R.J., Casale, G., Quillan, K.R., Fraser, K.L., and Bebell, T.G., 2018, Kinematic, deformational, and thermochronologic conditions along the Goswin Lead and Fries shear zones: Constraining the western-eastern Blue Ridge boundary in northwestern North Carolina: Tectonics, v. 37, no. 10, p. 3500–3523. [Also available at <https://doi.org/10.1029/2017TC004879>.]

Merschat, A.J., Carter, M.W., Odom, W.E., and McAleer, R.J., 2023a, Geologic map of the Sparta East, Sparta West, and parts of the Glade Valley and Whitehead 7.5-minute quadrangles, North Carolina and Virginia [abs.]: Geological Society of America Abstracts with Programs, v. 55, no. 2. [Also available at <https://doi.org/10.1130/abs/2023SE-385969>.]

Merschat, A.J., Carter, M.W., Scheip, C.M., Wooten, R.M., Owen, L.A., Douglas, T.J., Figueiredo, P.M., Cattannach, B.L., Stewart, K.G., Hill, J.S., and Witt, A.C., 2020, Surface rupture from the 9 August 2020, Mw 5.1 Sparta, North Carolina earthquake and connections with bedrock geology [abs.]: Geological Society of America Abstracts with Programs, v. 52, no. 6. [Also available at https://www.researchgate.net/publication/346587714_SURFACE_RUPTURE_FROM_THE_9_AUGUST_2020_MW_5.1_SPARTA_NORTH_CAROLINA_EARTHQUAKE_AND_CONNECTIONS_WITH_BEDROCK_GEOLOGY.]

Merschat, A.J., Southworth, S., Holm-Denoma, C.S., and McAleer, R.J., 2016, Geology of the Mount Rogers area, revisited—Evidence of Neoproterozoic continental rifting, glaciation, and the opening and closing of the Iapetus ocean, Blue Ridge, VA–NC–TN, in Merschat, A.J., ed., Geology of the Mount Rogers area, revisited, Blue Ridge, VA–NC–TN: Carolina Geological Society Annual Field Trip Guidebook, October 29–30, 2016, p. 3–28. [Also available at https://carolinageologicalsociety.org/2016_files/CGS2016%20guidebook_complete.pdf.]

Merschat, A.J., Weinmann, B.R., and Carter, M.W., 2023b, Database for the preliminary map of the surface rupture from the August 9, 2020, Mw 5.1 earthquake near Sparta, North Carolina—The Little River fault and other possible coseismic features: U.S. Geological Survey data release, <https://doi.org/10.5066/955SPGHH>.

Rankin, D.W., Espenshade, G.H., and Neuman, R.B., 1972, Geologic map of the west half of the Winston–Salem quadrangle, North Carolina, Virginia, and Tennessee: U.S. Geological Survey Miscellaneous Geologic Investigations Map I-709–A, 1 sheet, scale 1:250,000. [Also available at <https://doi.org/10.3133/I709A>.]

Raymond, L.A., 2015, Formal revision of the Ashe and Alligator Back Formation names: Southeastern Geology, v. 51, no. 3, p. 135–143. [Also available at https://www.researchgate.net/publication/311437170_Formal_revision_of_the_Ashe_and_Alligator_Back_Formation_names.]

U.S. Geological Survey, 2020, 3DEP Lidar Explorer—Lidar results [NC SpartaEQ 1 2020, LPC link]: U.S. Geological Survey, The National Map lidar database, accessed in 2022, at <https://apps.nationalmap.gov/lidar-explorer/#> [direct link to dataset is https://rockyweb.usgs.gov/delivery/Datasets/Staged/Elevation/LPC/Projects/NC_SpartaEarthquake_2020_D21/NC_SpartaEQ_1_2020/].

U.S. Geological Survey National Cooperative Geologic Mapping Program, 2020, GEMS (Geologic Map Schema)—A standard format for the digital publication of maps: U.S. Geological Survey Techniques and Methods, book 11, chap. B10, 74 p., accessed February 10, 2023, at <https://doi.org/10.3133/t11B10>.

U.S. Geological Survey, 2022, Earthquake Hazards Program—Search earthquake catalog: U.S. Geological Survey database, accessed March 18, 2022, at <https://earthquake.usgs.gov/earthquakes/search/>.

U.S. Geological Survey, [undated], Topographic data quality levels (QLs)—Table 1: U.S. Geological Survey, 3D Elevation Program web page, accessed in 2022, at <https://www.usgs.gov/3d-elevation-program/topographic-data-quality-levels-qls>.

ISSN 2231-1258 (online)
<https://doi.org/10.3133/ofr20231074>

Any use of trade, firm, or product names is for descriptive purposes only and does not imply endorsement by the U.S. Government.

For sale by U.S. Geological Survey, Box 25286, Denver Federal Center, Denver, CO 80225; <https://store.usgs.gov/>; 1-888-ASK-USGS (1-888-275-8747).

Suggested citation: Merschat, A.J., and Carter, M.W., 2023, Preliminary map of the surface rupture from the August 9, 2020, Mw 5.1 earthquake near Sparta, North Carolina—The Little River fault and other possible coseismic features: U.S. Geological Survey Open-File Report 2023-1074, 1 sheet, scale 1:24,000, <https://doi.org/10.3133/ofr20231074>.

Associated data for this publication: Merschat, A.J., Weinmann, B.R., and Carter, M.W., 2023, Database for the preliminary map of the surface rupture from the August 9, 2020, Mw 5.1 earthquake near Sparta, North Carolina—The Little River fault and other possible coseismic features: U.S. Geological Survey data release, <https://doi.org/10.5066/955SPGHH>.